

Noname manuscript No.
 (will be inserted by the editor)

A constrained optimization trajectory method using normalized gradients

Long Chen · Wenyi Chen · Kai-Uwe Bletzinger

Received: date / Accepted: date

Abstract We present a first-order method using normalized response gradients for constrained optimization problems. The method is consistently derived from our previous work, a modified search direction method developed for inequality constrained optimization problems that applies the singular-value decomposition (SVD). In the SVD-modified search direction method, a search direction is designed as a descent direction of the objective function. The resulting optimization trajectory converges to the central path of the interior-point method. The method has shown both efficiency and robustness in the industry-applicable structural optimization problems. However, there has been a lack of theory of the method, which this paper tries to address. Here, it will be shown that the formula for determining the search direction is surprisingly simple. The resulting optimization trajectory finds a local minimum for non-convex constrained optimization problems. We study the method in various examples, both analytically and numerically, and provide a convergence analysis of general 2D problems. An extension for general constrained optimization problems is given at the end of the paper, and an illustrative example is shown.

Keywords trajectory method · normalized gradients · non-convex constrained optimization · central path · nonlinear programming

L. Chen
 Technical University of Munich, Germany
 Tel.: +49 (89) 289 - 22462
 Fax: +49 (89) 289 - 22421
 E-mail: long.chen@tum.de

W. Chen
 Wuhan University, China
 E-mail: wychencn@whu.edu.cn

K.-U. Bletzinger
 Technical University of Munich, Germany
 E-mail: kub@tum.de

Mathematics Subject Classification (2010) 65K05 · 90C30 · 90C51

1 Introduction

In the field of engineering, unique difficulties occur that have prevented the general application of gradient-based optimization to design problems [20]. Optimization difficulties that we encounter when applying the structural optimization techniques for mechanical design problems [3] are:

- (i) the response functions and gradients are very expensive to evaluate. They often require finite element analysis of structures, computational fluid dynamics (CFD) for fluids, or fluid-structure interaction (FSI) for multi-physics problems.
- (ii) a very large number of design variables. The design space can be the full degrees of freedom of a finite element mesh.
- (iii) sometimes, a large number of constraints. For point-wise defined geometrically constrained or element-wise based stress constrained design optimization, the number of constraints can be very large despite the cheap computation of each response.
- (iv) the complexity of setting up the design problem and its time-consuming solutions. We pursue, therefore, a method that provides feasible/usable design at each optimization iteration.
- (v) the design problem can be non-convex, and this is especially so when we have nonlinear constraint functions.

Motivated by the above-mentioned difficulties, in this paper, we discuss the design and analysis of a new first-order method for solving the nonlinear constrained optimization problem

$$\begin{aligned}
 & \text{minimize } f(x) \\
 & \text{subject to } g(x) \leq 0 \\
 & \quad h(x) = 0,
 \end{aligned} \tag{1}$$

where $f : \mathbb{R}^n \rightarrow \mathbb{R}$, $g : \mathbb{R}^n \rightarrow \mathbb{R}^m$, and $h : \mathbb{R}^n \rightarrow \mathbb{R}^p$ are smooth functions. The method is consistently derived from our recent work [7] that uses normalized response gradients and singular-value decomposition to compute a search direction for the inequality constrained optimization problems. The SVD-modified search direction method was successfully applied for industrial structural optimization problems with a large number of design variables and constraints. Good efficiency and robustness are shown (some examples can be found in [7]). However, its underlying theory remains unclear, which we try to address here. In the present work, we present a simpler form of this method and extend it to solve general constrained optimization problems. We study the method both analytically and numerically to understand the behavior of the present method. Based on our results, we give a convergence analysis of 2D problems.

The present method uses normalized response gradients to compute a search direction that is a descent direction of the objective function. A key characteristic of the present method is that the resulting optimization trajectory converges to the central path of the logarithmic barrier interior-point method. A literature review of the interior-point method is, therefore, given. In 1956, Frisch introduced the logarithmic barrier function method [11], which may be considered one of the very first interior-point methods. It is, however, commonly recognized that the modern development of this class of methods started after the publication of the seminal paper of Karmarkar in 1984 [15]. Megiddo first described the framework for the primal-dual interior-point method in [16], and this viewpoint was proved later to be very productive [26]. The predictor-corrector algorithm proposed by Mehrotra in [17] is considered one of the most successful practical implementations of the primal-dual framework, and serves as the basis of many later software. Around the year 2000, interest grew in developing interior-point methods for large-scale nonlinear programming problems. Byrd et al. introduced a trust-region framework for nonlinear programming in [5]. Fletcher and Leyffer proposed filter methods for nonlinear programming in [9], and this filter approach was adapted to barrier methods in a number of ways [25]. Recently, various works have shown useful applications of the interior-point methods in machine learning [21]. For more comprehensive reviews of the interior-point methods, the reader is referred to [10][18], and more recently, in [12].

In the field of engineering, the interior-point method is among the most popular choices [1]. It can be found in truss design optimization [14], in optimization of differential algebraic equation systems in process engineering [6], and in topology optimization [13], just to name a few. In the field of structural engineering, the method of moving asymptotes proposed by Svanberg [24] and the evolutionary method developed by Xie and Stephen [27] are probably the most widely used methods for design optimization problems. Both methods are, however, not classical gradient-based methods.

Another key characteristic of the present method is the usage of normalized gradients. To the best of the authors' knowledge, no literature discusses an interior-point method that applies normalized response gradients. In [22], Stander and Snyman present a feasible direction method that applies normalized gradients. Their work is then continued and further developed in [8] and [23]. In these works, the active-set strategy is used. The common idea is to formulate a linear system under given input criteria on a chosen working set of (active) constraints, and a feasible search direction is obtained by solving the linear system. In the present method, we use the logarithmic barrier function to treat multiple inequality constraints, and no linear system needs to be solved for determining the search direction. Thus, it also differs with most known interior-point methods, in which a Newton problem is solved at each optimization iteration. This unusual characteristic strongly motivates the work of the present paper.

The paper is structured as follows: First, a short review of the logarithmic barrier function method and the related central path condition is given. We

then propose the simple form of the present method for single inequality constrained optimization problems. After that, we show analytical and numerical examples and study the behavior of the present method. Based on this, we give a convergence analysis of general 2D problems. Then, we present the general formulation for multiple inequality constrained optimization problems and the extension to general constrained optimization problems. Finally, we give the conclusion and outlook of the paper.

2 A short review of the logarithmic barrier function method and the introduction of the normalized central path condition

As the basis of the present method, we shortly review the logarithmic barrier function and the central path condition in this section. Following [4], we consider optimization problems that includes inequality constraints,

$$\begin{aligned} & \text{minimize} && f(x) \\ & \text{subject to} && g_i(x) \leq 0, \quad i = 1, \dots, m \end{aligned} \quad (2)$$

where $f, g_1, \dots, g_m : \mathbb{R}^n \rightarrow \mathbb{R}$ are twice differentiable. The general constrained optimization will be discussed in the section 7.

The idea of the logarithmic barrier function method is to approximately formulate the inequality constrained problem (2) as an equality constrained problem to which Newton's method can be applied [4]. The logarithmic barrier for the problem (2) is defined as,

$$\Phi(x) = - \sum_{i=1}^m \log(-g_i(x)), \quad i = 1, \dots, m \quad (3)$$

and the approximated problem is given as,

$$\begin{aligned} & \text{minimize} && f(x) + \frac{1}{t} \Phi(x) \\ & && = f(x) + \frac{1}{t} \sum_{i=1}^m -\log(-g_i(x)) \end{aligned} \quad (4)$$

where t is a positive parameter. The logarithmic barrier (3) grows without bound if $g_i(x) \rightarrow 0$.

The *central path* associated with problem (2) solving with logarithmic barrier method is defined as the set of points $x^*(t)$, $t > 0$, which are called *central points*. The necessary and sufficient conditions, which characterize points on the central path, are

$$\begin{aligned} 0 &= \nabla f(x^*(t)) + \frac{1}{t} \nabla \Phi(x^*(t)) \\ &= \nabla f(x^*(t)) + \frac{1}{t} \sum_{i=1}^m \frac{1}{-g_i(x^*(t))} \nabla g_i(x^*(t)) \end{aligned} \quad (5)$$

By normalizing the gradient of the objective and the logarithmic barrier function, we can rewrite the central path condition as

$$\frac{\nabla f}{|\nabla f|} + \frac{\nabla \Phi}{|\nabla \Phi|} = 0, \quad (6)$$

which we call the *normalized central path condition*. $|\cdot|$ denotes the Euclidean norm. Note that by normalizing the gradients, the path parameter t has vanished. The condition 6 characterizes the central path, which differs with 5 that characterizes rather a point on the central path. In particular, for optimization problems with a single inequality constraint, the *normalized central path condition* reads as

$$\frac{\nabla f}{|\nabla f|} + \frac{\nabla g}{|\nabla g|} = 0. \quad (7)$$

The *normalized central path condition* is used in section 5 for the convergence analysis.

3 The optimization trajectory method for single inequality constrained optimizations

In this section, we present the search direction for single inequality constrained optimization problems. We present a simple formula that is derived based on our previous work [7]. We then show an optimization example and solve it analytically.

3.1 The formula for computing the search direction

In the present method, a search direction at each iteration is computed using the normalized objective and constraint gradient as

$$\mathbf{s}_\zeta = -\frac{\nabla f}{|\nabla f|} - \zeta \frac{\nabla g}{|\nabla g|}, \quad (8)$$

where $\zeta \in [0, 1]$ is the only parameter that controls the search direction. The formulation is very simple, and it is closely related to equation 7, which defines the *normalized central path condition*. Obviously, 8 computes a descent direction of the objective function due to the nature of the normalized vector. The search direction reduces to the normalized steepest descent direction of the objective function when $\zeta = 0$ is chosen.

The search direction 8 is derived from the SVD-modified search direction method that is introduced in our previous work [7]. In the following, we briefly review the SVD-modified search direction method and then show the derivation. The idea behind the design of the search direction is presented in [7], and the interested reader may refer to it for more details.

In the SVD-modified search direction method, at each iteration, we construct a sensitivity matrix \mathbf{m} as

$$\mathbf{m} = \begin{pmatrix} \frac{\nabla f}{|\nabla f|} \\ \frac{\nabla g}{|\nabla g|} \end{pmatrix}. \quad (9)$$

The change in the objective function df and the constraint function dg resulting from an arbitrary design change $dx \in \mathbb{R}^n$ read as

$$\begin{aligned} df &= \nabla f dx, \\ dg &= \nabla g dx. \end{aligned} \quad (10)$$

We obtain an input-output system using the sensitivity matrix \mathbf{m} as

$$\begin{pmatrix} \frac{df}{|\nabla f|} \\ \frac{dg}{|\nabla g|} \end{pmatrix} = \mathbf{m} dx, \quad (11)$$

We apply singular-value decomposition to the sensitivity matrix \mathbf{m} :

$$\mathbf{m} = \mathbf{U} \boldsymbol{\Sigma} \mathbf{V}^T = \sum_{i=1}^{\min(2,n)} \sigma_i \mathbf{u}_i \mathbf{v}_i^T \quad (12)$$

Thus, an orthonormal bases set \mathbf{v}_i , $i = 1, 2$ is obtained. Each \mathbf{v}_i can be used as a base search direction for the design update, and \mathbf{v}_1 and \mathbf{v}_2 are defined as follows:

- \mathbf{v}_1 : by taking $\delta\mathbf{v}_1$ as the design change, we obtain a change in objective as well as in constraint function $[\frac{df}{|\nabla f|}, \frac{dg}{|\nabla g|}]^T = \sigma_1 \delta\mathbf{u}_1$, which is a **decrease** in the objective function and an **increase** in the constraint function.
- \mathbf{v}_2 : by taking $\delta\mathbf{v}_2$ as the design change, we obtain a change in the objective as well as in the constraint function $[\frac{df}{|\nabla f|}, \frac{dg}{|\nabla g|}]^T = \sigma_2 \delta\mathbf{u}_2$, which is a **decrease** in the objective function and a **decrease** in the constraint function.

It is interesting to note that the design vector $\delta\mathbf{v}_1$ provides a similar result as the filter approach presented in [9], which tries to minimize the so-called bi-objective optimization problem with two goals of minimizing the objective function f and the constraint violation $|g|$.

With \mathbf{v}_1 and \mathbf{v}_2 , we can then rewrite the normalized steepest descent direction $-\frac{\nabla f}{|\nabla f|}$ as

$$-\frac{\nabla f}{|\nabla f|} = \cos \alpha_1 \mathbf{v}_1^T + \cos \alpha_2 \mathbf{v}_2^T, \quad (13)$$

where α_1 is the angle between \mathbf{v}_1^T and $-\frac{\nabla f}{|\nabla f|}$, and α_2 is the angle between \mathbf{v}_2^T and $-\frac{\nabla f}{|\nabla f|}$. The SVD-modified search direction introduced in [7] reads

$$\mathbf{s}_c = \cos \alpha_1 \mathbf{v}_1^T + c \cdot \cos \alpha_2 \mathbf{v}_2^T, \quad (14)$$

where $c \geq 1$ is introduced to enlarge the contribution of the design mode \mathbf{v}_2 .

In the following, we show the derivation of 8 from 14. According to SVD and the definition of \mathbf{v}_1 and \mathbf{v}_2 , we have

$$\begin{aligned}\mathbf{v}_1^T &= \frac{1}{\sqrt{2-2\cos\theta}} \left(-\frac{\nabla f}{|\nabla f|} + \frac{\nabla g}{|\nabla g|} \right) \\ \mathbf{v}_2^T &= \frac{1}{\sqrt{2+2\cos\theta}} \left(-\frac{\nabla f}{|\nabla f|} - \frac{\nabla g}{|\nabla g|} \right),\end{aligned}\quad (15)$$

where θ is the angle between the objective function gradient ∇f and the constraint function gradient ∇g . With θ we also have

$$\begin{aligned}\cos \alpha_1 &= - \left\langle \frac{\nabla f}{|\nabla f|}, \mathbf{v}_1^T \right\rangle = \frac{\sqrt{1-\cos\theta}}{\sqrt{2}}, \\ \cos \alpha_2 &= - \left\langle \frac{\nabla f}{|\nabla f|}, \mathbf{v}_2^T \right\rangle = \frac{\sqrt{1+\cos\theta}}{\sqrt{2}}.\end{aligned}\quad (16)$$

Inserting 15 and 16 into 14 we have

$$\mathbf{s}_c = -\frac{\nabla f}{|\nabla f|} - \frac{(c-1)}{2} \left(\frac{\nabla f}{|\nabla f|} + \frac{\nabla g}{|\nabla g|} \right). \quad (17)$$

As we are only interested in the direction of the vector field \mathbf{s}_c , we can rewrite it as

$$\mathbf{s}_\zeta = -\frac{\nabla f}{|\nabla f|} - \zeta \frac{\nabla g}{|\nabla g|},$$

with $\zeta = \frac{c-1}{c+1}$. With $c \in [1, +\infty)$ we have $\zeta \in [0, 1)$.

3.2 An analytical 2D optimization example

We show a 2D optimization problem and solve it analytically with the optimization trajectory by integrating the search direction field 8. The optimization problem reads,

$$\begin{aligned}\text{minimize } f(x_1, x_2) &= \frac{1}{2}(x_1^2 + x_2^2) \\ \text{subject to } g(x_1, x_2) &= -x_2 + 10 \leq 0,\end{aligned}\quad (18)$$

The present search direction field \mathbf{s}_ζ reads,

$$\begin{aligned}\mathbf{s}_\zeta &= -\frac{\nabla f}{|\nabla f|} - \zeta \frac{\nabla g}{|\nabla g|} \\ &= \frac{-1}{\sqrt{x_1^2 + x_2^2}} \left\{ x_1, x_2 - \zeta \sqrt{x_1^2 + x_2^2} \right\}.\end{aligned}\quad (19)$$

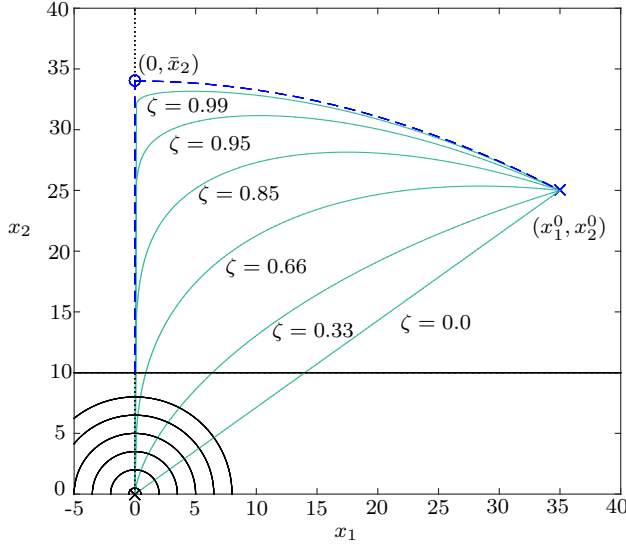


Fig. 1 Optimization trajectories for the 2D linear constrained optimization problem 18 with different parameter ζ . The black circles show the objective function contours. The black line is the constraint function. The dotted line shows the central path. As $\zeta \rightarrow 1^-$, a part of the trajectory Γ^ζ based on the present search direction field \mathbf{s}_ζ (8) converges to the central path.

We define an initial design as (x_1^0, x_2^0) . Let $\bar{x}_2 = \frac{1}{2} \left(x_2^0 + \sqrt{(x_1^0)^2 + (x_2^0)^2} \right)$, then, the trajectory Γ^ζ of the present search direction field \mathbf{s}_ζ is

$$x_2 + \sqrt{x_1^2 + x_2^2} = 2\bar{x}_2 \left| \frac{x_1}{x_1^0} \right|^{1-\zeta}. \quad (20)$$

Let $(x_{1,\zeta}, x_{2,\zeta})$ be a point on the trajectory Γ^ζ with a maximal x_2 component, then we have

$$(x_{2,\zeta})^\zeta = \frac{2}{1+\zeta} \frac{\bar{x}_2}{|x_1^0|^{1-\zeta}} \left(\frac{\sqrt{1-\zeta^2}}{\zeta} \right)^{1-\zeta}, \quad (21)$$

and

$$|x_{1,\zeta}| = \frac{\bar{x}_2}{\zeta} \sqrt{1-\zeta^2}. \quad (22)$$

Let $\zeta \rightarrow 1^-$, then, $x_{1,\zeta} \rightarrow 0$, $x_{2,\zeta} \rightarrow \bar{x}_2$, the trajectory Γ^ζ will converge to the curve Γ that is a union of the parabola

$$x_1^2 = 4\bar{x}_2^2 - 4x_2\bar{x}_2, \quad x_1 \in (0, x_1^0) \quad (\text{or } (x_1^0, 0)) \quad (23)$$

and the interval $(0, \bar{x}_2)$ on x_2 -axis. In figure 1 we show the parabola starting from the initial design (x_1^0, x_2^0) and reaches $(0, \bar{x}_2)$, which lays on the central

path illustrated as a dotted line. As $\zeta \rightarrow 1^-$, a part of the trajectory T^ζ converges to the central path.

As $\bar{x}_2 = \frac{1}{2} \left(x_2^0 + \sqrt{(x_1^0)^2 + (x_2^0)^2} \right)$, we have $\bar{x}_2 \geq x_2^0$. This means for any feasible initial design, as $\zeta \rightarrow 1^-$, the resulting optimization trajectory always reaches first a close neighborhood of the central path (at the point $(0, \bar{x}_2)$), where it is further away from the constraint compared to the initial design. It then follows the central path and reaches the optimal solution.

The behavior of the trajectory can also be understood via the SVD-modified search direction approach presented in section 3.1. As $\zeta \rightarrow 1^-$, $c \rightarrow +\infty$, the design mode \mathbf{v}_2 is dominant in formula 14. According to the definition, a design change in the direction of \mathbf{v}_2 leads to both decrements in objective and constraint function, and thus the optimization trajectory travels further away from the constraint. After the optimization trajectory reaches a close neighborhood of the central path, the effect of the parameter c is reduced significantly by the term $\cos \alpha_2$ as it tends to be 0. The optimization trajectory then follows the central path to reach the optimal solution.

4 Numerical studies

In this section, we show numerical studies for the present search direction field 8. First, we propose a computational algorithm for the present optimization trajectory method. Then, we study it in various examples. Based on the studies, we try to get more insight into the behavior of the present optimization trajectory.

4.1 The computational algorithm for single inequality constraint

For simplicity, we use fixed step sizes in all of the computational algorithms and thus neglect the line search method since we want to focus the study on the search direction. In our numerical studies, we choose adequately small step sizes to better represent the analytical trajectory based on the present search direction field. Nevertheless, it is noteworthy that our computational experiences show that even a fixed step size method with well-chosen parameter ζ provides robust solutions in industrial applications of structural optimization problems (some examples are shown in [7]).

For the computational algorithm, we give the stopping criteria as:

- Stopping criterion I: when $f(x^{(k)}) > f(x^{(k-1)})$. In this case, we assume that a local minimum of the objective function is found inside the feasible domain.
- Stopping criterion II: when there is a violation of the inequality constraint $g \geq 0$.

We give a convergence criterion that is referred to the *normalized central path condition* defined in 7. As $\frac{\nabla f}{|\nabla f|} + \frac{\nabla g}{|\nabla g|} \rightarrow 0$, we have $\left\langle \frac{\nabla f}{|\nabla f|}, \frac{\nabla g}{|\nabla g|} \right\rangle + 1 \rightarrow 0$.

For a small number $\epsilon_1 > 0$ that defines the convergence parameter value, the convergence criterion for the algorithm is given as

$$\left\langle \frac{\nabla f}{|\nabla f|}, \frac{\nabla g}{|\nabla g|} \right\rangle + 1 < \epsilon_1 \quad (24)$$

for feasible designs.

In Algorithm 1, we sketch a computational algorithm for single inequality constrained optimizations with a fixed step size.

Algorithm 1 The computational algorithm with a fixed step size for single inequality constrained optimizations

Step 1. Set $k = 0$. Start with an initial feasible design $\mathbf{x}^{(0)}$. Select a parameter $\zeta \in [0, 1)$, a fixed step size α , and a parameter ϵ_1 for the convergence check.

Step 2. Compute the objective and inequality constraint function values and their gradients. Check the stopping criteria I and II. If the criterion I is satisfied, then stop. If the criterion II is satisfied, stop and go to Step 4. Otherwise, compute the search direction $\mathbf{d}^{(k)}$ with 8.

Step 3. Set $\mathbf{x}^{(k+1)} = \mathbf{x}^{(k)} + \alpha \frac{\mathbf{d}^{(k)}}{|\mathbf{d}^{(k)}|}$. Update the iteration counter as $k = k + 1$, and go to Step 2.

Step 4. Check for convergence $\left\langle \frac{\nabla f}{|\nabla f|}, \frac{\nabla g}{|\nabla g|} \right\rangle + 1 < \epsilon_1$.

Remarks.

- The Algorithm 1 gives a basic algorithm that aims to study the behavior of the present search direction field. The chosen step size directly affects the efficiency of the algorithm.
- To better represent the analytical optimization trajectory, it is suggested to choose a small step size α by large parameter ζ . This can be understood via the formulation 8, as $\zeta \rightarrow 1^-$, $|\mathbf{s}_\zeta| \rightarrow 0$ at the central path.
- For practical implementations, a suitable line search method might be needed, and methods that adapt the parameter ζ during the optimization process can increase the efficiency. These two options are not included in the actual paper.
- If the convergence check in Step 4 is not satisfied, one can either restart the optimization at the design $\mathbf{x}^{(k-1)}$ with a larger parameter ζ or to switch to a method of the active-set strategy, to find a local optimum.

4.2 Numerical experiments

We report numerical experiments for single constrained optimization problems. We show three constrained optimization examples that apply Algorithm 1:

1. Minimizing an elliptic objective function that is subjected to a linear constraint,

$$\begin{aligned} & \text{minimize } f(x_1, x_2) = x_1^2 + x_1 x_2 + \frac{1}{2} x_2^2 \\ & \text{subject to } g(x_1, x_2) = -x_1 - x_2 + 15 \leq 0. \end{aligned} \quad (25)$$

2. Minimizing an elliptic objective function that is subjected to a quadratic constraint,

$$\begin{aligned} & \text{minimize } f(x_1, x_2) = x_1^2 + x_1 x_2 + \frac{1}{2} x_2^2 \\ & \text{subject to } g(x_1, x_2) = \frac{1}{10}(x_1 - 20)^2 - x_2 - 5 \leq 0. \end{aligned} \quad (26)$$

3. Minimizing a quadratic objective function that is subjected to a non-convex quadratic constraint,

$$\begin{aligned} & \text{minimize } f(x_1, x_2) = (x_1 - 2)^2 + (x_2 - 2)^2 \\ & \text{subject to } g(x_1, x_2) = -\frac{1}{10}(x_1 - 3)^2 - x_2 + 3 \leq 0. \end{aligned} \quad (27)$$

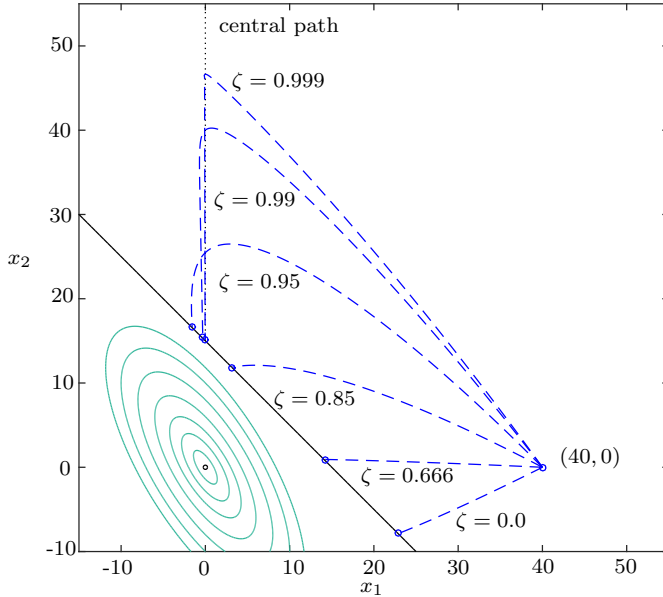


Fig. 2 Optimization trajectories for the 2D linear constrained optimization problem 25 with different parameter ζ . The circles are the contours of the objective function. The black line is the constraint function. The dotted black line is the central path. As $\zeta \rightarrow 1^-$, a part of the trajectory Γ^ζ based on the present search direction field \mathbf{s}_ζ (8) converges to the central path.

In figures 2 and 3, we show the optimization trajectories for examples 25 and 26, respectively. As $\zeta \rightarrow 1^-$, a part of the optimization trajectory, which is illustrated as the dashed line, converges to the central path. The central paths are illustrated as dotted lines. The objective value decreases steadily while the optimization proceeds and a solution close to the local optimum is found when the inequality constraint becomes active.

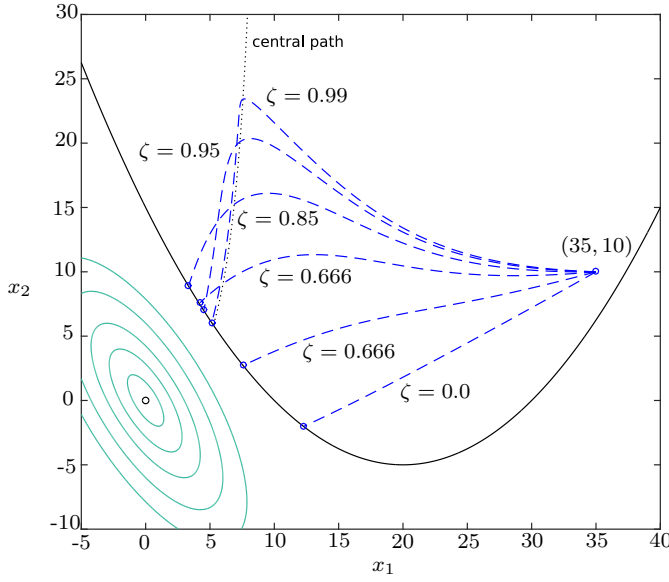


Fig. 3 Optimization trajectories for the 2D nonlinear constrained optimization problem 26 with different parameter ζ . The circles are the contours of the objective function. The black curve is the constraint function. The dotted black line is the central path. As $\zeta \rightarrow 1^-$, a part of the trajectory Γ^ζ based on the present search direction field s_ζ (8) converges to the central path.

In example 18 of the previous section, at a central point, the tangent direction of the central path is parallel with the objective gradient direction. In example 25, although the central path remains a straight line, the tangent direction of the central path differs from the objective gradient direction. Despite this, the result of the numerical optimization shows that the optimization trajectory still follows the central path, and it converges to it as $\zeta \rightarrow 1^-$. In the second example 26, the central path is nonlinear as is shown in figure 3. The obtained optimization trajectories are still able to approach and follow the central path, and eventually, they reach designs that are close to the analytical optimal solution.

In figure 4, we show the results of example 27 that has a non-convex constraint. The problem has two central paths due to the non-convexity. Similar to the last two examples 25 and 26, as $\zeta \rightarrow 1^-$, the optimization trajectory converges to the central path(s). As the optimization proceeds, the objective function value decreases, and the optimization trajectory leaves the central path on the top right and approaches the central path on the bottom left. It then follows that central path and finds a solution close to the analytical solution. The behavior of this example is studied more closely in the following.

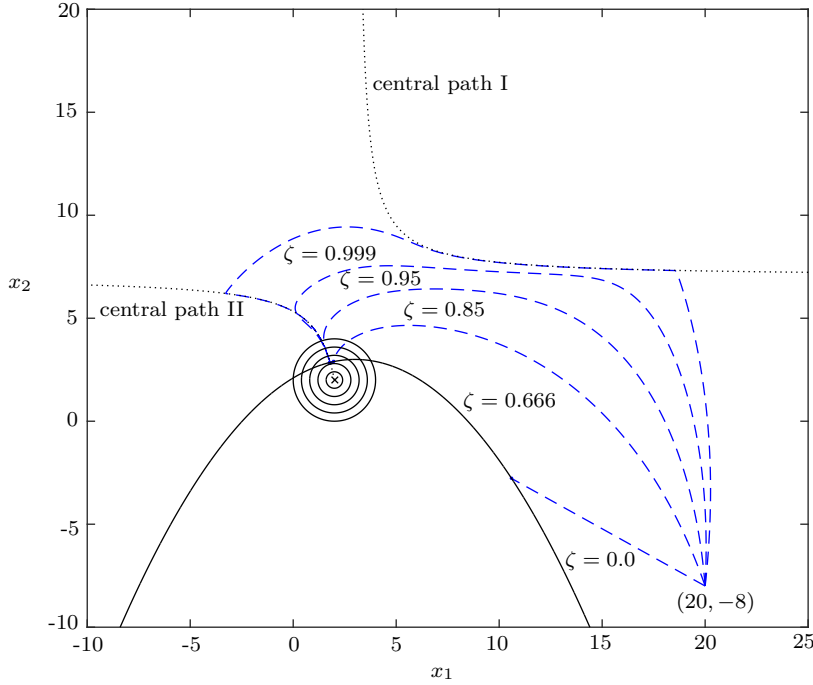


Fig. 4 Optimization trajectories for the 2D non-convex constrained optimization problem 27 with different parameter ζ . The black circles show the objective function contours. The black line is the constraint function. The dotted black line is the central path. As $\zeta \rightarrow 1^-$, parts of the trajectory Γ^ζ based on the present search direction field \mathbf{s}_ζ (8) converges to the central paths.

4.3 A study on the behavior of the optimization trajectory

We show a further study of example 27. Based on it, we try to explain the behavior of the present trajectory method. In figure 5, we plot the optimization result with $\zeta = 0.9999$ together with a few depicted contours of both the objective function and the constraint function.

We plot three points A, B, and C on the central path, where the plotted contours of the objective and constraint function are tangent to each other. We choose an initial design \mathbf{x}^0 that is close to the point A. It can be observed: instead of heading to the left side of the central path, the optimization trajectory finds its way to the right side. It then follows the central path, but leaves at point C and reaches the other central path. It eventually finds the optimal solution by following this central path. Along the optimization trajectory, the objective function value decreases steadily. The question is now, why does the optimization trajectory choose one side (point B side) of the same central

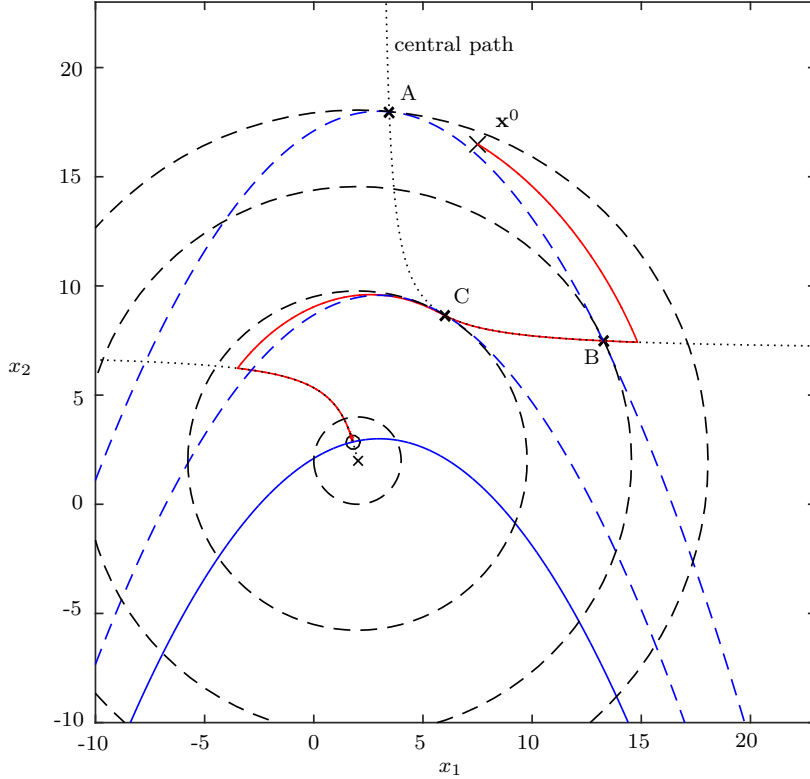


Fig. 5 A study on the behavior of the optimization trajectory for problem 27. Red curve is the optimization trajectory. Black dashed circles are the contours of the objective function, while the blue dashed curves show the contours of the constraint function. The dotted black lines are the central paths.

path over another (point A side)? The answer may lie in the difference in the curvatures of the contours of the objective and constraint function between point A and B. We observe the following fact:

Let $\frac{\nabla f}{\|\nabla f\|}$ be the normal vector of the contours of objective and constraint function at the central path, κ_f be the curvature of the objective function, and κ_g be the curvature of the constraint function, then

- at point A: $\kappa_f - \kappa_g > 0$.
- at point B: $\kappa_f - \kappa_g < 0$.

Based on this observation, we infer the behavior of the optimization trajectory: The optimization trajectory is able to find and follow a central path, on which the central point satisfies the condition

$$\kappa_f - \kappa_g < 0. \quad (28)$$

We call condition 28 the *relative convex condition*. This behavior can also be used to explain why the optimization trajectory leaves the central path at point C, where $\kappa_f = \kappa_g$, and heads towards another central path. In the next section, we give a convergence analysis based on the *relative convex condition*.

5 Convergence analysis of 2D problems

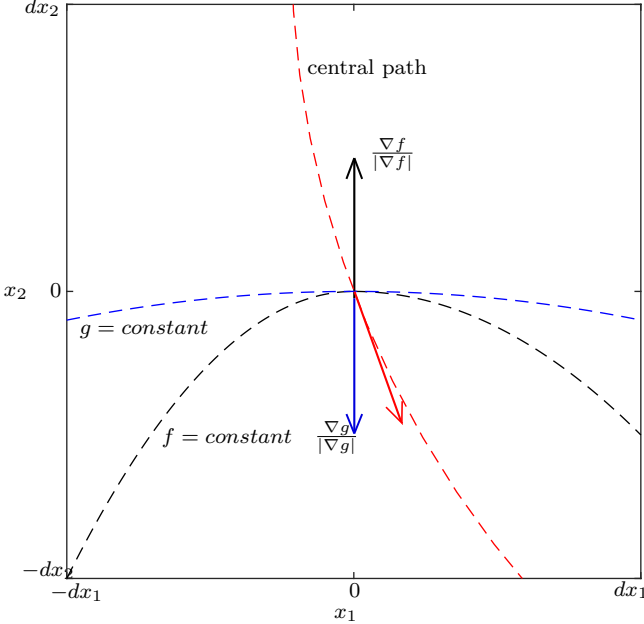


Fig. 6 Illustration for the convergence analysis for general 2D problems

Consider the following 2D optimization problem that is illustrated in figure 6,

$$\begin{aligned} & \text{minimize } f(x_1, x_2) \\ & \text{subject to } g(x_1, x_2) \leq 0. \end{aligned} \quad (29)$$

Taking a point on the central path, say $(0, 0)$, we have

$$\begin{aligned} \frac{\nabla f}{|\nabla f|} \Big|_{(0,0)} &= \{0, 1\}, \\ \frac{\nabla g}{|\nabla g|} \Big|_{(0,0)} &= \{0, -1\}. \end{aligned} \quad (30)$$

Thus, $f(x_1, x_2) = c_1$ determines a function that we denote as $x_2 = \phi(x_1)$; $g(x_1, x_2) = c_2$ determines a function that we denote as $x_2 = \psi(x_1)$. Therefore

we have $f(x_1, \phi(x_1)) = c_1, \forall x_1$, and $\phi(0) = 0$. Deriving $f(x_1, \phi(x_1))$ w.r.t. x_1 , we get $\frac{\partial f}{\partial x_1} + \frac{\partial f}{\partial x_2} \phi'(x_1) = 0$. So we have

$$\phi'(x_1) = -\frac{\partial_{x_1} f}{\partial_{x_2} f}.$$

At $(0, 0)$, $\phi'(0) = 0$, which means the tangent direction is parallel with the x_1 -axis. The second order derivative ϕ'' determines the shape of the function ϕ , i.e.,

$$\kappa_f = \phi''(0) = -\frac{f_{x_1 x_1}(0, 0)}{f_{x_2}(0, 0)}. \quad (31)$$

Similarly,

$$\kappa_g = \psi''(0) = -\frac{g_{x_1 x_1}(0, 0)}{g_{x_2}(0, 0)}. \quad (32)$$

According to 28 we have

$$-\frac{f_{x_1 x_1}(0, 0)}{f_{x_2}(0, 0)} < -\frac{g_{x_1 x_1}(0, 0)}{g_{x_2}(0, 0)}. \quad (33)$$

According to 30, we have

$$\begin{aligned} f_{x_2}(0, 0) &= |\nabla f(0, 0)|, \\ g_{x_2}(0, 0) &= -|\nabla g(0, 0)|. \end{aligned} \quad (34)$$

We then have

$$\frac{f_{x_1 x_1}(0, 0)}{|\nabla f(0, 0)|} > -\frac{g_{x_1 x_1}(0, 0)}{|\nabla g(0, 0)|}, \quad (35)$$

or

$$\frac{f_{x_1 x_1}(0, 0)}{|\nabla f(0, 0)|} + \frac{g_{x_1 x_1}(0, 0)}{|\nabla g(0, 0)|} > 0. \quad (36)$$

$\frac{\nabla f}{|\nabla f|}$ has two entries, resulting in four entries when derived with respect to x_1, x_2 . $\frac{f_{x_2}}{|\nabla f|}$ has the maximum value 1 at $(0, 0)$, resulting its two derivatives are 0. Thus, the Jacobian Matrix for $\frac{\nabla f}{|\nabla f|}$ at the origin reads

$$\begin{bmatrix} \frac{\partial}{\partial x_1} \left(\frac{f_{x_1}}{|\nabla f|} \right) & \frac{\partial}{\partial x_2} \left(\frac{f_{x_1}}{|\nabla f|} \right) \\ \frac{\partial}{\partial x_1} \left(\frac{f_{x_2}}{|\nabla f|} \right) & \frac{\partial}{\partial x_2} \left(\frac{f_{x_2}}{|\nabla f|} \right) \end{bmatrix} = \begin{bmatrix} \frac{f_{x_1 x_1}}{|\nabla f|} & \frac{\partial}{\partial x_2} \left(\frac{f_{x_1}}{|\nabla f|} \right) \\ 0 & 0 \end{bmatrix}. \quad (37)$$

Similarly, the Jacobian Matrix at the origin for $\frac{\nabla g}{|\nabla g|}$ reads

$$\begin{bmatrix} \frac{\partial}{\partial x_1} \left(\frac{g_{x_1}}{|\nabla g|} \right) & \frac{\partial}{\partial x_2} \left(\frac{g_{x_1}}{|\nabla g|} \right) \\ \frac{\partial}{\partial x_1} \left(\frac{g_{x_2}}{|\nabla g|} \right) & \frac{\partial}{\partial x_2} \left(\frac{g_{x_2}}{|\nabla g|} \right) \end{bmatrix} = \begin{bmatrix} \frac{g_{x_1 x_1}}{|\nabla g|} & \frac{\partial}{\partial x_2} \left(\frac{g_{x_1}}{|\nabla g|} \right) \\ 0 & 0 \end{bmatrix}. \quad (38)$$

We denote

$$\lambda = \frac{f_{x_1 x_1}}{|\nabla f|} + \frac{g_{x_1 x_1}}{|\nabla g|}, \quad (39)$$

and

$$\mu = \frac{\partial}{\partial x_2} \left(\frac{f_{x_1}}{|\nabla f|} \right) + \frac{\partial}{\partial x_2} \left(\frac{g_{x_1}}{|\nabla g|} \right). \quad (40)$$

Since $\frac{\nabla f}{|\nabla f|} + \frac{\nabla g}{|\nabla g|} = 0$ represents the central path, the tangent of the central path, which is illustrated as the red arrow in figure 6, reads

$$\lambda x_1 + \mu x_2 = 0. \quad (41)$$

The Taylor series of the negative search direction $\frac{\nabla f}{|\nabla f|} + \zeta \frac{\nabla g}{|\nabla g|}$ at the origin reads

$$\begin{aligned} \frac{\nabla f}{|\nabla f|} + \zeta \frac{\nabla g}{|\nabla g|} &= \{0, 1 - \zeta\} + \{\lambda x_1 + \mu x_2, 0\} \\ &\quad + (\zeta - 1) \left\{ \frac{g_{x_1 x_1}}{|\nabla g|} x_1 + \frac{\partial}{\partial x_2} \left(\frac{g_{x_1}}{|\nabla g|} \right) x_2, 0 \right\} + o(\rho). \end{aligned} \quad (42)$$

with $\rho = \sqrt{x_1^2 + x_2^2}$. We denote $\frac{g_{x_1 x_1}}{|\nabla g|} = a$ and $\frac{\partial}{\partial x_2} \left(\frac{g_{x_1}}{|\nabla g|} \right) = b$. Then we have the differential equation neglecting the higher-order terms for the search path as

$$\begin{cases} \frac{dx_1}{dt} = -(\lambda x_1 + \mu x_2) + (1 - \zeta)(ax_1 + bx_2), \\ \frac{dx_2}{dt} = -(1 - \zeta). \end{cases} \quad (43)$$

Given an initial point (x_1^0, x_2^0) , we have

$$x_2(t) = x_2^0 - (1 - \zeta)t. \quad (44)$$

Therefore,

$$\frac{dx_1}{dt} = -(\lambda - (1 - \zeta)a)x_1 + (-\mu + (1 - \zeta)b)(x_2^0 - (1 - \zeta)t). \quad (45)$$

The equation 45 has the solution

$$x_1(t) = x_1^0 e^{-(\lambda - (1 - \zeta)a)t} + \frac{-\mu + (1 - \zeta)b}{\lambda - (1 - \zeta)a} x_2(t) + \frac{-\mu + (1 - \zeta)b}{[\lambda - (1 - \zeta)a]^2} (1 - \zeta). \quad (46)$$

46 is the approximated optimization trajectory neglecting higher-order terms. Since $\lambda > 0$, if $1 - \zeta$ is small enough, $\lambda - (1 - \zeta)a > \frac{\lambda}{2} > 0$. If $t \rightarrow +\infty$, solution 46 converges to the line

$$x_1 = \frac{-\mu + (1 - \zeta)b}{\lambda - (1 - \zeta)a} x_2 + \frac{-\mu + (1 - \zeta)b}{[\lambda - (1 - \zeta)a]^2} (1 - \zeta). \quad (47)$$

The line 47 approaches the tangent of the central path $x_1 = \frac{-\mu}{\lambda} x_2$ with an error depending on $(1 - \zeta)$.

Let $\zeta \rightarrow 1^-$, to guarantee $x_2(t) = x_2^0 - (1 - \zeta)t$ stays close to $(0, 0)$, we need $t \sim \frac{c_0}{1 - \zeta} \rightarrow +\infty$. And then equation 46 converges to

$$x_1(t) = -\frac{\mu}{\lambda} x_2(t), \quad (48)$$

which is the tangent of the central path as in 41. The order of error is $(1 - \zeta)$. Thus, it confirms our numerical observations shown in the previous section. The optimization trajectory is able to find and follow a central path where the *relative convex condition* (28) is satisfied.

6 The optimization trajectory method for multiple inequality constraints

In this section, we discuss the generalization of the present method for multiple inequality constraints. The generalization was first proposed in [7]. In the present paper, we deduce the method in a different way that is based on the convergence analysis of the optimization trajectory shown in section 5.

6.1 The formula for multiple inequality constraints

In the previous section, we show that for single inequality constrained optimization problems, as $\zeta \rightarrow 1^-$, the optimization trajectory based on the search direction

$$\mathbf{s}_\zeta = -\frac{\nabla f}{|\nabla f|} - \zeta \frac{\nabla g}{|\nabla g|}, \quad \zeta \in [0, 1),$$

converges to the central path with the *normalized central path condition*

$$\frac{\nabla f}{|\nabla f|} + \frac{\nabla g}{|\nabla g|} = 0.$$

For multiple inequality constrained optimization, we can approximate the original problem 2 with logarithmic barrier method as is shown in 4. The resulting *normalized central path condition* reads

$$\frac{\nabla f}{|\nabla f|} + \frac{\nabla \Phi}{|\nabla \Phi|} = 0.$$

Thus, in the same way, we can write the search direction for the logarithmic barrier approximated optimization problem as

$$\mathbf{s}_\zeta = -\frac{\nabla f}{|\nabla f|} - \zeta \frac{\nabla \Phi}{|\nabla \Phi|}, \quad \zeta \in [0, 1), \quad (49)$$

with $\Phi = -\sum_{i=1}^m \log(-g_i)$ that can be just considered as a single function. Note that the parameter t for the logarithmic barrier method has vanished in formula 49. The search direction obtained by 49 is a descent direction of the objective function due to the nature of the normalized vector.

In Algorithm 2, we sketch a computational algorithm for multiple inequality constrained optimization that is a slightly modified version of the algorithm 1. The stopping criteria are the same as described in subsection 4.1. The convergence criterion is updated as

$$< \frac{\nabla f}{|\nabla f|}, \frac{\nabla \Phi}{|\nabla \Phi|} > +1 < \epsilon_1. \quad (50)$$

Algorithm 2 The computational algorithm with a fixed step size for multiple inequality constrained optimizations

Step 1. Set $k = 0$. Start with an initial feasible design $\mathbf{x}^{(0)}$. Select a parameter $\zeta \in [0, 1)$, a fixed step size α , and a parameter ϵ_1 for the convergence check.

Step 2. Compute the objective and inequality constraint function values and their gradients. Check the stopping criteria I and II. If the criterion I is satisfied, then stop. If the criterion II is satisfied, stop and go to Step 4. Otherwise, compute the search direction $\mathbf{d}^{(k)}$ with 49.

Step 3. Set $\mathbf{x}^{(k+1)} = \mathbf{x}^{(k)} + \alpha \frac{\mathbf{d}^{(k)}}{|\mathbf{d}^{(k)}|}$. Update the iteration counter as $k = k + 1$, and go to Step 2.

Step 4. Check for convergence $\left\langle \frac{\nabla f}{|\nabla f|}, \frac{\nabla \Phi}{|\nabla \Phi|} \right\rangle + 1 < \epsilon_1$.

6.2 An example with multiple constraints

We demonstrate the Algorithm 2 with a linear programming problem that is introduced in [2]:

Minimize

$$f = -440x_1 - 600x_2, \quad (51)$$

which is subjected to the inequality constraints g_i , with $i = 1$ to 5 :

$$\begin{aligned} g_1 &= x_1 + x_2 - 16 \leq 0, \\ g_2 &= \frac{1}{28}x_1 + \frac{1}{14}x_2 - 1 \leq 0, \\ g_3 &= \frac{1}{14}x_1 + \frac{1}{24} - 1 \leq 0, \\ g_4 &= -x_1 \leq 0, \\ g_5 &= -x_2 \leq 0. \end{aligned} \quad (52)$$

The result is shown in figure 7 with the parameter $\zeta = 0.99$. The method is able to find the optimum, which is the vertex joined by the constraint g_1 and g_2 . Note that the present method can also be applied to nonlinear programming problems with multiple inequality constraints as shown in [7].

7 The optimization trajectory for general constrained optimization problems

In this section, we give an extension of the present method for the general constrained optimization problem that is defined in 1. The idea is to treat the inequality constraints and equality constraints separately. Starting with a feasible design, we project the objective gradient and the inequality constraint gradients onto the equality constraint hyperplane and apply formula 49 to the projected gradients to compute the search direction. Any violation of the equality constraints is then treated in the next step so that the design becomes feasible again. In this way, we reach a local minimum iteratively by following the equality constraints under the guidance of the present search direction considering the inequalities.

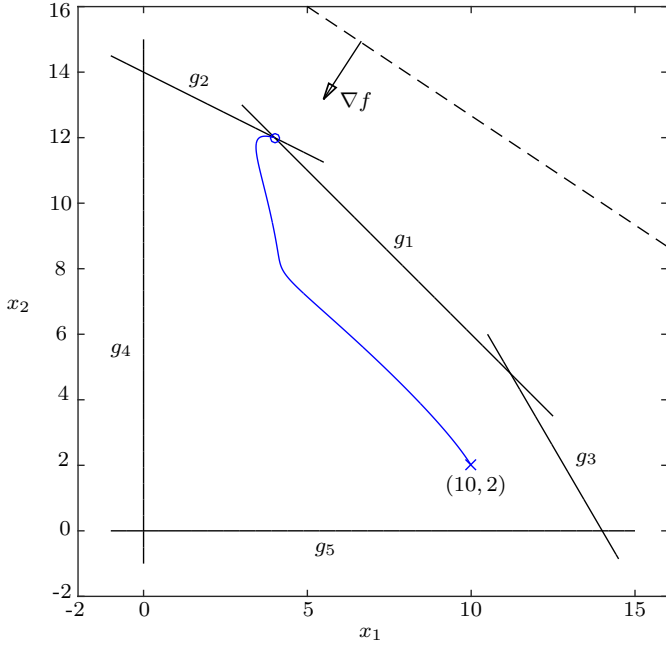


Fig. 7 The optimization trajectory starting from an initial design $(10, 2)$ for the problem 51-52 is shown in blue curve. The method uses the parameter $\zeta = 0.99$. The black dashed line shows the contour line of the objective functions; the remaining black lines show the different constraint functions.

7.1 Projected search direction on the null space of the linearized equality constraints

In the present work, we adopt Rosen's gradient projection method [19] to treat equality constraints. For the general constrained optimization problem 1 that is approximated with the logarithmic barrier function, following [4], we can write its central path condition as

$$\begin{aligned} 0 &= t\nabla f + \nabla\Phi + \mu^T A \\ &= t\nabla f + \sum_{i=1}^m \frac{1}{-g_i} \nabla g_i + \sum_{i=1}^p \mu_i \nabla h_i, \end{aligned} \quad (53)$$

where μ are the dual variables for the equality constraints, and $A_{ij} = \partial_j h_i$ is the Jacobian matrix of the equality constraint function $h(x)$. We project equation 53 onto the null space of the equalities

$$\text{Null}(A) = \{w \mid Aw = 0\}.$$

We denote d_n as the projected vector of the vector d onto the null space $\text{Null}(A)$. The projection can be done with the following equation

$$d_n = (\mathbf{I} - A^T (A A^T)^{-1} A) d. \quad (54)$$

Obviously, the projections of the vectors ∇h_i onto the null space $\text{Null}(A)$ are zero. Therefore, we get the null space projected central path condition as

$$\begin{aligned} 0 &= t \nabla f_n + \sum_{i=1}^m \frac{1}{-g_i} \nabla g_{in} \\ &= t \nabla f_n + \nabla \Phi_n. \end{aligned} \quad (55)$$

Normalizing the gradients we get

$$0 = \frac{\nabla f_n}{|\nabla f_n|} + \frac{\nabla \Phi_n}{|\nabla \Phi_n|}, \quad (56)$$

and thus we get the null space projected search direction formula

$$\mathbf{s}_{\zeta n} = -\frac{\nabla f_n}{|\nabla f_n|} - \zeta \frac{\nabla \Phi_n}{|\nabla \Phi_n|}, \quad \zeta \in [0, 1]. \quad (57)$$

Since we have linearized the equality constraint $h(x)$, it is inevitable that errors may occur for equality constraints after taking one null space step using the search direction 57. This error can be corrected iteratively to a specified tolerance ϵ_h using the following range space calculation

$$d_r = -A^T (AA^T)^{-1} h(x), \quad (58)$$

where $h(x)$ are the equality constraint function values at each sub-iteration.

7.2 The computational algorithm for general constrained optimization

In Algorithm 3, we sketch a basic computational algorithm for general constrained optimizations based on the discussion above. The stopping criteria for the algorithm are the same as presented in section 4.1. The convergence criterion is slightly modified according to 56 as

$$< \frac{\nabla f_n}{|\nabla f_n|}, \frac{\nabla \Phi_n}{|\nabla \Phi_n|} > +1 < \epsilon_1. \quad (59)$$

Remark. For multiple inequality constrained optimizations, at Step 4, we can first calculate the gradient of the logarithmic barrier $\nabla \Phi$ and then project it onto the null space using 54. Thus, at each iteration, instead of calculating projections for every single inequality gradient, only two projections have to be done: one for the objective function gradient and the other for the logarithmic barrier gradient.

Algorithm 3 The computational algorithm with a fixed step size for general constrained optimizations.

Step 1. Set $k = 0$. Start with an initial feasible design $\mathbf{x}^{(0)}$. Select a parameter $\zeta \in [0, 1)$, a fixed step size α , a parameter ϵ_1 for the convergence check, and a parameter ϵ_h as the tolerance for the equality constraints.

Step 2. At design $\mathbf{x}^{(k)}$, compute the equality constraint function values and check the constraint violation. If the tolerance ϵ_h is satisfied, go to Step 4.

Step 3. Compute the equality constraint gradients. Update the design $\mathbf{x}^{(k)}$ iteratively with 58, until the equality constraint violation satisfies the tolerance ϵ_h .

Step 4. Compute the objective and inequality constraint function values and gradients. Project the response gradients onto the null space of the equality constraints with 54. Check the stopping criteria I and II. If the criterion I is satisfied, then stop. If the criterion II is satisfied, stop and go to Step 6. Otherwise, compute the search direction $\mathbf{d}^{(k)}$ with 57.

Step 5. Set $\mathbf{x}^{(k+1)} = \mathbf{x}^{(k)} + \alpha \frac{\mathbf{d}^{(k)}}{|\mathbf{d}^{(k)}|}$. Update the iteration counter as $k = k + 1$, and go to Step 2.

Step 6. Stop and check for convergence with 59.

7.3 An example for general constrained optimization

The proposed algorithm is tested on various analytical examples. In this section we show a demonstrating example. The general constrained optimization reads,

$$\begin{aligned}
 & \text{minimize } f(x, y, z) = z \\
 & \text{subject to } g_1(x, y, z) = -\frac{1}{2}x - \frac{3}{4}y - z - \frac{1}{2} \leq 0, \\
 & \quad g_2(x, y, z) = -\frac{1}{2}x + \frac{3}{4}y - z - \frac{1}{2} \leq 0, \\
 & \quad h(x, y, z) = x^2 + y^2 + z^2 - 1 = 0.
 \end{aligned} \tag{60}$$

The present optimization problem is non-convex, and it has two local optimal solutions. In figures 8 and 9, we show two optimization results starting at the same initial design $(x, y, z) = (-0.7, 0.15, 0.7)$, but with different parameters $\zeta = 0.9$ and $\zeta = 0.999$, respectively. It is very interesting to see that different parameters ζ lead to different local optimal solutions. In this case, two central paths lead to two different local optima due to the non-convexity of the problem. Different parameters ζ result in different search directions, which in turn influence the optimization results by converging to different central paths. The larger parameter ζ leads to a better optimal solution. We report this example because this phenomenon can be observed in some non-convex optimization problems, depending on the chosen initial design. Our computational experiences tend to confirm that a larger ζ leads to a better local solution when multiple local solutions can be found. Further studies on this phenomenon might be of interest in future works.

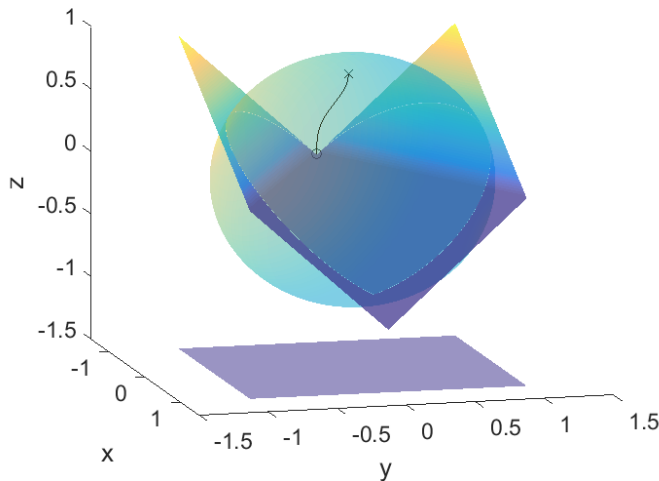


Fig. 8 Optimization trajectory for the 3D general constrained optimization problem 60 with the parameter $\zeta = 0.9$.

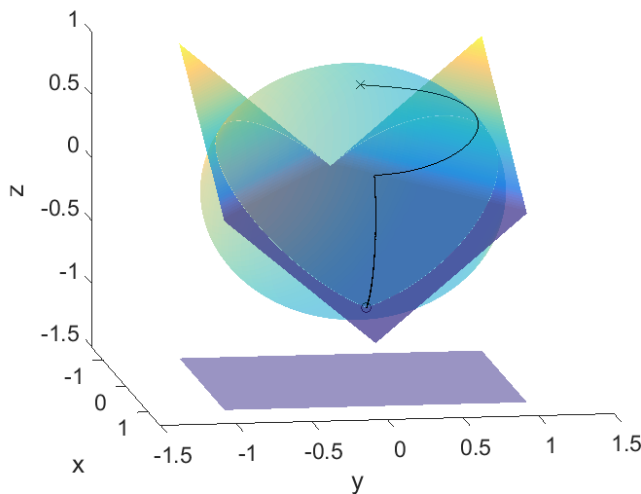


Fig. 9 Optimization trajectory for the 3D general constrained optimization problem 60 with the parameter $\zeta = 0.999$.

8 Conclusions and outlook

In this work, we present a constrained optimization trajectory method using normalized response gradients for nonlinear programming problems. The calculation of the search direction does not require the solution of a linear system, and the resulting optimization trajectory shows a similar behavior to the interior-point method. In the actual paper, our main contributions are:

1. Present the simple form of the method.
2. Study the behavior of the present optimization trajectory and give a convergence analysis of 2D problems.
3. Extend the method for general optimization problems that include equality constraints.

The present method can be enhanced in adding the line search method and implement methods that can adapt the parameter ζ . Based on this work, we would like to present a mathematical analysis for the global behavior and convergence of high-dimensional problems in the subsequent paper.

9 Acknowledgment

The work by the first author is done during his work as one of the coordinators at the Bavarian Graduate School of Computational Engineering (BGCE) as a part of the Elite Network of Bavaria. The working experiences and financial support is gratefully acknowledged. The authors also thank Jian Cui from the Helmholtz Pioneer Campus for his generosity in proofreading this manuscript.

References

1. Arora, J., Wang, Q.: Review of formulations for structural and mechanical system optimization. *Structural and Multidisciplinary Optimization* **30**(4), 251–272 (2005). DOI 10.1007/s00158-004-0509-6
2. Arora, J.S.: *Introduction to optimum design*, 3rd edn. Elsevier (2011)
3. Bletzinger, K.U.: Shape optimization. In: *Encyclopedia of Computational Mechanics*, 2nd edn. Wiley (2018)
4. Boyd, S., Vandenberghe, L.: *Convex optimization*. Cambridge university press (2004)
5. Byrd, R.H., Gilbert, J.C., Nocedal, J.: A trust region method based on interior point techniques for nonlinear programming. *Mathematical programming* **89**(1), 149–185 (2000). DOI 10.1007/PL00011391
6. Cervantes, A.M., Wächter, A., Tütüncü, R.H., Biegler, L.T.: A reduced space interior point strategy for optimization of differential algebraic systems. *Computers & Chemical Engineering* **24**(1), 39–51 (2000). DOI 10.1016/S0098-1354(00)00302-1
7. Chen, L., Bletzinger, K., Geiser, A., Wüchner, R.: A modified search direction method for inequality constrained optimization problems using the singular-value decomposition of normalized response gradients. *Structural and Multidisciplinary Optimization* (2019). DOI 10.1007/s00158-019-02320-9
8. De Klerk, E., Snyman, J., Group, S.O.R., et al.: A feasible descent cone method for linearly constrained minimization problems. *Computers & Mathematics with Applications* **28**(6), 33–44 (1994). DOI 10.1016/0898-1221(94)00150-2
9. Fletcher, R., Leyffer, S.: Nonlinear programming without a penalty function. *Mathematical programming* **91**(2), 239–269 (2002). DOI 10.1007/s101070100244
10. Forsgren, A., Gill, P.E., Wright, M.H.: Interior methods for nonlinear optimization. *SIAM review* **44**(4), 525–597 (2002). DOI 10.1137/S0036144502414942
11. Frisch, R.: La résolution des problèmes de programme linéaire par la méthode du potentiel logarithmique. *Cahiers du Séminaire D'Econometrie* pp. 7–23 (1956). DOI 10.2307/20075373
12. Gondzio, J.: Interior point methods 25 years later. *European Journal of Operational Research* **218**(3), 587–601 (2012). DOI 10.1016/j.ejor.2011.09.017

13. Hoppe, R.H., Petrova, S.I., Schulz, V.: Primal-dual newton-type interior-point method for topology optimization. *Journal of Optimization Theory and Applications* **114**(3), 545–571 (2002). DOI 10.1023/A:1016070928600
14. Jarre, F., Kocvara, M., Zowe, J.: Optimal truss design by interior-point methods. *SIAM Journal on Optimization* **8**(4), 1084–1107 (1998). DOI 10.1137/S1052623496297097
15. Karmarkar, N.: A new polynomial-time algorithm for linear programming. *Combinatorica* **4**(4), 373–395 (1984). DOI 10.1007/BF02579150
16. Megiddo, N.: Pathways to the optimal set in linear programming. In: *Progress in mathematical programming*, pp. 131–158. Springer (1989)
17. Mehrotra, S.: On the implementation of a primal-dual interior point method. *SIAM Journal on optimization* **2**(4), 575–601 (1992). DOI 10.1137/0802028
18. Potra, F.A., Wright, S.J.: Interior-point methods. *Journal of Computational and Applied Mathematics* **124**(1-2), 281–302 (2000). DOI 10.1016/S0377-0427(00)00433-7
19. Rosen, J.: The gradient projection method for nonlinear programming. part ii. nonlinear constraints. *Journal of the Society for Industrial and Applied Mathematics* **9**(4), 514–532 (1961)
20. Snyman, J.A., Wilke, D.N.: New gradient-based trajectory and approximation methods. In: *Practical Mathematical Optimization*, pp. 197–250. Springer (2018)
21. Sra, S., Nowozin, S., Wright, S.J.: *Optimization for machine learning*. Mit Press (2012)
22. Stander, N., Snyman, J.: A new first-order interior feasible direction method for structural optimization. *International journal for numerical methods in engineering* **36**(23), 4009–4025 (1993). DOI 10.1002/nme.1620362306
23. Stander, N., Snyman, J., Coster, J.: On the robustness and efficiency of the sam algorithm for structural optimization. *International Journal for Numerical Methods in Engineering* **38**(1), 119–135 (1995). DOI 10.1002/nme.1620380108
24. Svanberg, K.: The method of moving asymptotes a new method for structural optimization. *International journal for numerical methods in engineering* **24**(2), 359–373 (1987). DOI 10.1002/nme.1620240207
25. Wächter, A., Biegler, L.T.: On the implementation of an interior-point filter line-search algorithm for large-scale nonlinear programming. *Mathematical programming* **106**(1), 25–57 (2006). DOI 10.1007/s10107-004-0559-y
26. Wright, S.J.: Primal-dual interior-point methods, vol. 54. Siam (1997)
27. Xie, Y.M., Steven, G.P.: A simple evolutionary procedure for structural optimization. *Computers & structures* **49**(5), 885–896 (1993). DOI 10.1016/0045-7949(93)90035-C